Electromagnetic Response of a Vortex in Layered Superconductors

Matthias Eschrig, J. A. Sauls

Department of Physics & Astronomy, Northwestern University, Evanston, IL 60208, USA

D. Rainer

Physikalisches Institut, Universität Bayreuth, D-95440 Bayreuth, Germany

We calculate the response of a vortex core in a layered superconductor to *ac* electromagnetic fields with frequencies $\omega \lesssim 2\Delta/\hbar$. In this frequency range the response is dominated by order parameter collective modes which are coupled to the vortex-core bound states of Caroli, de Gennes and Matricon. Our calculations show that a vortex core has a more complex and richer dynamics than predicted by previous theories. The *ac* field drives an oscillating, nearly homogeneous supercurrent in the direction of the electric field, superimposed with a dissipative current flow which has a dipolar spatial structure. The order parameter response at low frequencies is an approximately rigid collective motion of the vortex structure perpendicular to the external field. This structure becomes strongly deformed at frequencies of order $\omega \gtrsim 0.5\Delta/\hbar$. Coupling of the vortex-core bound states to collective modes of the order parameter at low frequencies leads to substantial enhancement of the dissipation near the vortex-center well above that of the normal-state.

Vortex cores play a key role in dissipation processes of superconductors in the Abrikosov phase. Bardeen and Stephen[1] modeled the vortex core as a region of normal metal in which the excitations in the core respond to an electromagnetic field like electrons in the normal metallic state. This is a good approximation for dirty superconductors with a mean free path, ℓ, much smaller than the coherence length ξ_0. However, in clean superconductors the low-lying excitations in the core are the bound states of Caroli, de Gennes and Matricon.[2] These excitations have superconducting and normal properties. They are the source of circulating supercurrents in the equilibrium vortex core,[3] and they are strongly coupled to the condensate by Andreev processes.[3,4] Their response to an electromagnetic field is radically different from that of normal electrons. For vortex cores one has two fundamentally different origins of dissipation. One is dissipation by the collective motion of the whole condensate, and the second is dissipation by transitions between Caroli-de Gennes-Matricon bound states. These processes are coupled because of the strong interaction between the condensate and the bound states, and requires a self-consistent treatment of condensate and bound-state dynamics. Earlier calculations neglected this coupling.[5,6] We present the first fully self-consistent calculation of the current response to an *ac* electric field, with frequencies comparable with the gap frequency $\Delta/\hbar$, in the vortex core. Our results show that self-consistency is essential for even a qualitative understanding of low-frequency dynamics and dissipation by the core.

We consider an s-wave superconductor with a random distribution of impurities in a static magnetic field. The applied *ac* electric field, $\delta\mathbf{E}(t) = -\frac{1}{c}\partial_t \delta\mathbf{A}(t)$, is linearly polarized in $\hat{\mathbf{x}}$-direction, and its wavelength is large compared to ξ_0. We assume an impurity scattering rate such that the superconductor is outside the super-clean limit; i.e. all bound states are broadened by an amount comparable to or larger than the "mini-gap",

Δ^2/E_f.[2] We investigate the intermediate clean regime, $\xi_0 \lesssim \ell \lesssim (E_f/\Delta)\xi_0$, where we expect the model of a "normal metal core" to break down. In the intermediate clean range we can use the quasiclassical theory of Fermi liquid superconductivity formulated by Eilenberger,[7] Larkin and Ovchinnikov,[8] and Eliashberg,[9] which is a powerful method for studying non-equilibrium superconductivity.

The numerical solution of nonequilibrium transport problems is greatly simplified by a new formulation of the nonequilibrium quasiclassical equations. Two of the new transport equations are a generalization of the Riccati-type equilibrium equations of Nagato et al.,[10] and Schopohl and Maki.[11] We present the central equations of the theory and refer readers to Ref. 12 for notation, their derivation and the connection to the quasiclassical Green's functions.

The scalar transport equations for the distribution functions, $\gamma^{R,A}$, $\tilde{\gamma}^{R,A}$, x^K, $\tilde{x}^K$, which are functions of momentum $\mathbf{p}_f$, position $\mathbf{R}$, energy ϵ, and time t, are

$$i\hbar\,\mathbf{v}_f \cdot \boldsymbol{\nabla}\gamma^{R,A} + 2\epsilon\gamma^{R,A} = -\gamma^{R,A} \otimes \tilde{\Delta}^{R,A} \otimes \gamma^{R,A} +$$
$$v^{R,A} \otimes \gamma^{R,A} - \gamma^{R,A} \otimes \tilde{v}^{R,A} - \Delta^{R,A} \tag{1}$$

$$i\hbar\,\mathbf{v}_f \cdot \boldsymbol{\nabla}\tilde{\gamma}^{R,A} - 2\epsilon\tilde{\gamma}^{R,A} = -\tilde{\gamma}^{R,A} \otimes \Delta^{R,A} \otimes \tilde{\gamma}^{R,A} +$$
$$\tilde{v}^{R,A} \otimes \tilde{\gamma}^{R,A} - \tilde{\gamma}^{R,A} \otimes v^{R,A} - \tilde{\Delta}^{R,A} \tag{2}$$

$$i\hbar\,\mathbf{v}_f \cdot \boldsymbol{\nabla}x^K + i\hbar\,\partial_t x^K +$$
$$\left(\gamma^R \otimes \tilde{\Delta}^R - v^R\right) \otimes x^K + x^K \otimes \left(\Delta^A \otimes \tilde{\gamma}^A + v^A\right) =$$
$$\gamma^R \otimes \tilde{v}^K \otimes \tilde{\gamma}^A - \Delta^K \otimes \tilde{\gamma}^A - \gamma^R \otimes \tilde{\Delta}^K - v^K \tag{3}$$

$$i\hbar\,\mathbf{v}_f \cdot \boldsymbol{\nabla}\tilde{x}^K - i\hbar\,\partial_t \tilde{x}^K +$$
$$\left(\tilde{\gamma}^R \otimes \Delta^R - \tilde{v}^R\right) \otimes \tilde{x}^K + \tilde{x}^K \otimes \left(\tilde{\Delta}^A \otimes \gamma^A + \tilde{v}^A\right) =$$
$$\tilde{\gamma}^R \otimes v^K \otimes \gamma^A - \tilde{\Delta}^K \otimes \gamma^A - \tilde{\gamma}^R \otimes \Delta^K - \tilde{v}^K. \tag{4}$$

External fields, the superconducting order parameter and impurity scattering enter the transport equations as driving fields and scattering integrals through the self-energies, $v^{R,A,K}$, $\tilde{v}^{R,A,K}$, $\Delta^{R,A,K}$, and $\tilde{\Delta}^{R,A,K}$. These

self energies are functionals of the distribution functions and must be determined self-consistently. Equations (1-4), together with the self-energy equations, are numerically stable and are the basis for efficient numerical algorithms for solving nonequilibrium problems in the quasiclassical theory of superconductivity. For the *ac* response of the vortex we linearize Eqs. (1-4) in the external field.[12] The linear response equations require as input the self-consistent equilibrium functions, $\gamma_{\text{eq}}^{R,A}$ and $\tilde{\gamma}_{\text{eq}}^{R,A}$, the order parameter and the impurity t-matrix for a pancake vortex. With these equilibrium solutions we then solve the first-order transport equations together with the linearized self-energy equations and the charge neutrality condition. The linearization is justified as long as the relation $e|\delta\mathbf{E}| \ll (\hbar\omega)^2/\Delta\xi_0$ holds.

The results presented below are calculated for a layered s-wave superconductor with a cylindrical Fermi surface along the $\hat{\mathbf{c}}$-direction, isotropic Fermi velocity $\mathbf{v}_f$ in the ab-plane, isotropic pairing interaction and a large Ginzburg-Landau parameter, $\kappa \gg 1$. Impurity scattering is taken into account self-consistently in the Born approximation. We consider a moderately clean superconductor with a long mean free path, $\ell = 10\xi_0$, where $\xi_0 = \hbar v_f/2\pi k_B T_c$ is the coherence length, and choose a low temperature, $T = 0.3 T_c$.
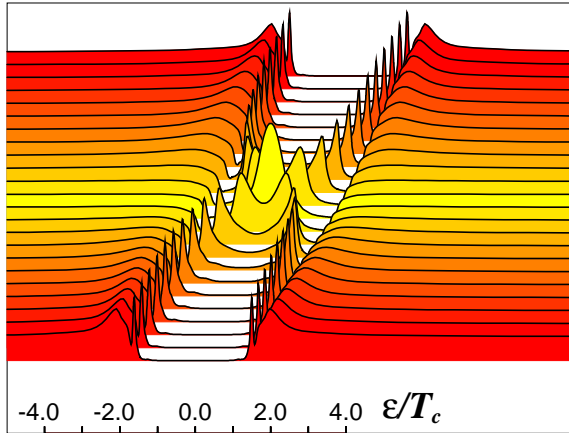

FIG. 1. Local density of states at different distances (up to $8.8\xi_0$, spacing $0.8\xi_0$) from the vortex center. The center of the vortex corresponds to the bright filled spectrum.

Fig. 1 shows the calculated local density of states of an equilibrium vortex at various distances from the core center. The important feature at the vortex center is the zero-energy bound state, which is broadened by impurity scattering into a resonance of width $\Gamma \approx 0.6 T_c$. At finite distances from the vortex center the bound states corresponding to different impact parameters of quasiclassical trajectories form a one-dimensional band, which is broadened by impurity scattering. The bands widen because of the coupling to the vortex flow field with increasing distance from the center, and develop Van Hove singularities at the band edges.
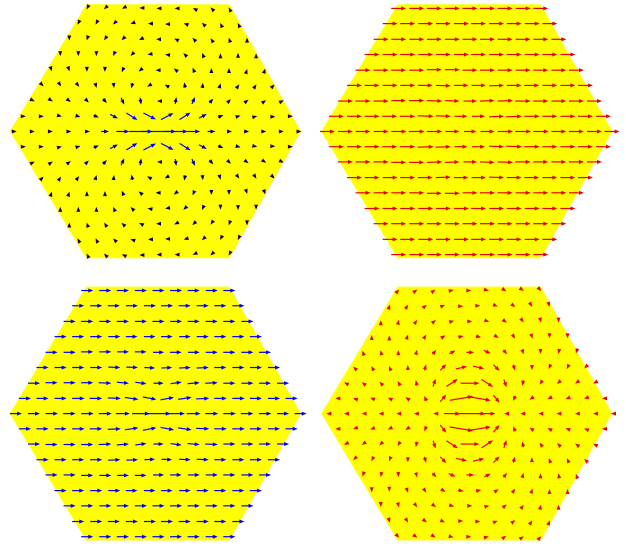

FIG. 2. Distribution of induced current density (left) and corresponding local electric field (right) in the vortex core at frequency $\omega = 0.3\Delta/\hbar$. The external electric field $\delta\mathbf{E}_\omega(t) = \delta\mathbf{E}_0 \cos\omega t$ points into $\hat{\mathbf{x}}$-direction. The top row is the dissipative response ($\sim \cos\omega t$), and the lower row is the reactive response ($\sim \sin\omega t$). Distances from the center extend up to $6.3\xi_0$.

Fig. 2 shows typical results for the current and field patterns induced by the external electric field, $\delta\mathbf{E}_\omega(t) = \delta\mathbf{E}_0 \cos\omega t$. The linear response decomposes into an *in-phase* ($\propto \cos\omega t$) and *out-of-phase* ($\propto \sin\omega t$) response. The in-phase current response at position $\mathbf{R}$ determines the local time-averaged energy transfer between the external field and the electrons, while the out-of-phase current response is non-dissipative. The in-phase and out-of-phase currents show characteristically different flow patterns. The non-dissipative current is nearly homogeneous (lower left), whereas the pattern of dissipative currents has qualitatively the form of a vortex-antivortex pair (upper left), which is consistent with a rigid shift in $\hat{\mathbf{y}}$-direction of the equilibrium current density. Additionally, this pattern is strongly deformed at higher frequencies (see Fig. 5 below). The right-hand side of Fig. 2 shows the total electric field, which consists of the homogeneous external field and the internal field due to charge fluctuations induced by the external field. Note that the induced field is predominantly out-of-phase and exceeds the external field in the center of the vortex core. For higher frequencies, $0.5\Delta \lesssim \hbar\omega \lesssim 2\Delta$, the induced dipolar field evolves from an out-of-phase dipole along the direction of the applied field to an in-phase dipole opposite to the applied field, thus reducing the external field by roughly one half. The induced field vanishes rapidly for frequencies above the gap edge. These features of the current response are robust and appear in all our calculations, independently of the temperature or mean free path. The charge density fluctuations responsible for the induced field are of the order $e\frac{\Delta}{E_f}\delta/\xi_0^2$, where $\delta = e \mid \delta\mathbf{E}_0 \mid \xi_0\Delta/(\hbar\omega)^2$ is a small dimensionless para-

meter that measures the amplitude of the perturbation. Thus, only a fraction $e\frac{\Delta}{E_f}\delta$ of an elementary charge accumulates periodically in time over an area of ξ_0^2, which is consistent with the condition of local charge neutrality.[13] Note that the induced charge in the vortex core resulting from particle-hole asymmetry, as discussed recently,[14] is of order $e(\frac{\Delta}{E_f})^2$. The in-plane current and field response (upper row of Fig. 2) shows that the local dissipation can be either positive ("hot spots" in which the in-phase current is parallel to the electric field), as well as negative ("cold spots" in which the dissipative current is anti-parallel to the electric field), and is dominated by dissipation in the vortex center. The net dissipation is positive, and is obtained by integrating $\mathbf{j}\cdot\mathbf{E}$ over the vortex. At higher frequencies the dissipation is dominated by higher energy bound states, and is less localized in the vicinity of the vortex center.

The electromagnetic response of the vortex-core is due to an interplay between collective dynamics of the order parameter and the dynamics of the Caroli-de Gennes-Matricon bound states. At frequencies below $0.5\Delta/\hbar$ the order parameter performs a nearly homogeneous oscillation perpendicular to the applied field, with a velocity that is 90° out of phase with the applied field. To show the deviations of the self-consistent order parameter from a rigidly oscillating vortex structure, on which all prior vortex dynamics calculations are based, we introduce the displacement vector $\delta\mathbf{R}_0(t)$ defined by $\delta\Delta(\mathbf{R},t)=\delta\mathbf{R}_0(\mathbf{R},t)\cdot\boldsymbol{\nabla}\Delta_0(\mathbf{R})$. The velocity field of the order parameter is then $\delta\mathbf{v}(\mathbf{R},t)=\partial_t\delta\mathbf{R}_0(\mathbf{R},t)$.
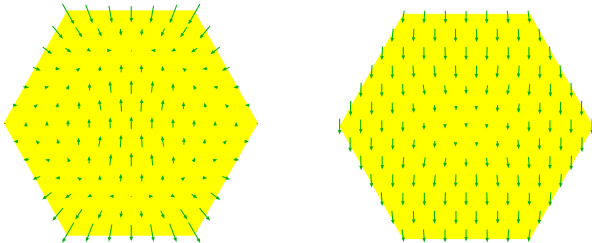

FIG. 3. Velocity field of the order parameter for $\omega=1.2\Delta/\hbar$, showing strong order parameter deformation. The left panel shows the in-phase motion of the velocity field, and the right panel shows the out-of-phase velocity. Distances from the center extend up to $4.7\xi_0$.

In Fig. 3 we show that the order parameter velocity field for $\omega=1.2\Delta/\hbar$ is strongly deformed. The vortex core is not rigid, but oscillates in-phase and perpendicular to the applied field. The velocity of the vortex center is of the order of $v_f\delta$, so the response is far from that of a stationary vortex. The amplitude of the vortex core oscillation increases with decreasing ω. However, for $\hbar\omega\gtrsim\Delta$, both the phase and amplitude of the vortex core oscillation decrease and approach zero above $\hbar\omega\sim2\Delta$.

The coupling between order parameter response and the bound states is demonstrated in Fig. 4, which compares the nonequilibrium spectral current density (re-

tarded Green's function, averaged with the weight v_{fx} over the Fermi surface) obtained from a self-consistent calculation with that obtained from a non-self-consistent calculation that takes into account the field-induced transitions within the band of Caroli-de Gennes-Matricon bound states, but freezes the order parameter degrees of freedom. The corresponding contribution to the current density is obtained by multiplying these functions by $-\frac{1}{2\pi}\tanh\frac{\epsilon-\omega/2}{2T}$ and integrating over ϵ.[15]
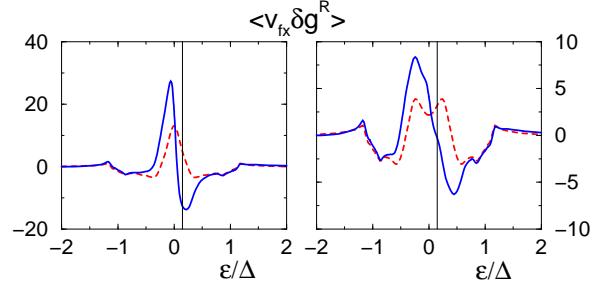

FIG. 4. Spectra for the dissipative part of the current density, $\langle v_{fx}\delta g^R\rangle$, at the vortex center (left) and at $0.8\xi_0$ in $\hat{\mathbf{x}}$-direction (right). The vertical lines correspond to $\epsilon=\omega/2$. The solid curves are the fully self-consistent spectral response. The dashed lines assume a frozen order parameter.

The dissipative part of the response function shows peaks in the spectral current density associated with the band of bound states in the vortex core. The spectral weight near $\epsilon=\omega/2$ does not contribute significantly to the current response. Fig. 4 shows that the bound state band is shifted to lower energy by the self-consistent response of the order parameter, leading to an enhanced dissipative current.
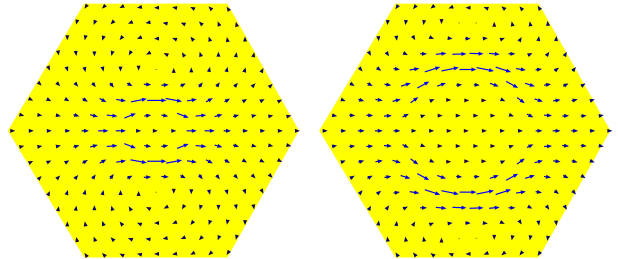

FIG. 5. Distribution of induced dissipative current density in the vortex core at frequencies $\omega=1.1\Delta/\hbar$ (left) and $1.5\Delta/\hbar$ (right). The current density at $\omega=1.5\Delta/\hbar$ is scaled by 2.5 relative to the current density at $1.1\Delta/\hbar$. Higher energy transitions between bound states produce dissipative currents at larger distances from the vortex center. Distances from the center extend up to $6.3\xi_0$.

The dissipative currents show nontrivial structure for frequencies in the range $\Delta<\hbar\omega<2\Delta$. Fig. 5 shows that the dissipative currents flow predominantly in regions where bound states with energy $\epsilon_{bs}=\hbar\omega/2$ are localized. We interpret these structures in terms of impurity-mediated transitions between the Van Hove band edges

(shown in Fig. 1) of the bound-state bands of the equilibrium vortex. The transition rate increases with decreasing frequency, and for $\hbar\omega$ comparable with the width of the zero energy bound state the dissipation is determined by the spectral dynamics of the zero energy bound states at the vortex center. The spectral response of these states (Fig. 4) leads to a dramatically enhanced dissipation near the vortex center, which is much larger than the normal-state dissipation.
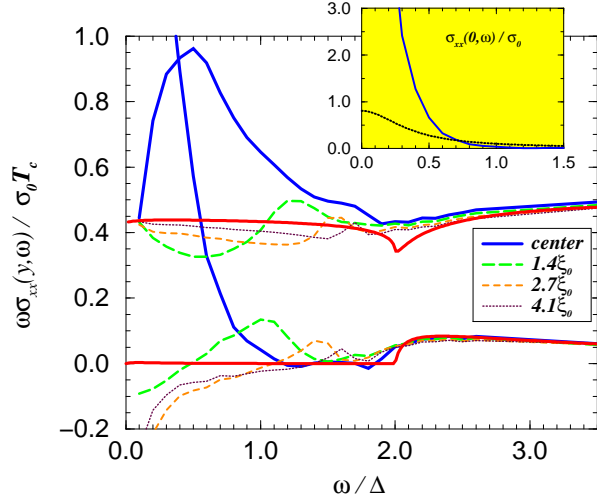

FIG. 6. Local conductivity of a vortex as a function of frequency. The lower set of curves shows $\omega\,\mathrm{Re}\sigma_{xx}$ as a function of distance from the center (shown in the legend) along the $\hat{\mathbf{y}}$ direction. The upper set of curves shows $\omega\mathrm{Im}\sigma_{xx}$. The thick red curves give the real and imaginary parts of the conductivity for a homogeneous superconductor with the same mean-free-path. The inset shows a comparison of the Drude absorption (black dotted) of a normal metal with the enhanced absorption at the center of the vortex core. Note that $\sigma_0 = 2e^2 N_f v_f^2$ and $\ell = 10\xi_0$.

Fig. 6 shows the conductivity in the vicinity of the vortex core as a function of frequency and distance from the vortex center. At the vortex center the real part of σ_{xx} (absorption) increases dramatically at low frequencies. Further away from the center the absorption is a maximum at a frequency corresponding to transitions between states near the Van Hove peaks of the bound state band. For comparison we show the conductivity of a homogeneous superconductor with the same mean-free path, which shows an absorption edge at $\hbar\omega = 2\Delta$. Also note that the low-frequency absorption in the vortex center is much larger than the Drude conductivity of the normal state (inset of Fig. 6). The conductivity sum-rule is obeyed; the apparent excess weight of $\int \mathrm{Re}\sigma_{xx}(\omega)d\omega$ is compensated by a negative delta function contribution associated with counterflowing supercurrents near the vortex center. Fig. 6 also shows the enhanced supercurrents in the vortex center, compared to those of a homogeneous superconductor, for frequencies comparable with the width of the states near zero-energy.

Finally we note that the order parameter response at low frequencies is mostly transverse to the electric field and that the dissipative current in the core is predominantly parallel to the applied field., i.e. there are no charge currents in $\hat{\mathbf{y}}$-direction related the order parameter motion. However, there is a substantial energy flux in the vortex core. Our calculations show, that the energy flux is predominantly in direction of the order parameter oscillation and confined in the vortex core within a few coherence lengths. The dipolar form of the dissipative current pattern leads to backflow currents far apart from the vortex core, which result locally in "cold spots". Thus, the states in the vortex core extract energy from the external field, and transport this energy several coherence lengths away from the vortex center in $\hat{\mathbf{y}}$-direction. The net absorption is determined by inelastic processes at the scale of the coherence length.

[1] J. Bardeen, M.J. Stephen, Phys. Rev. **140**, A1197 (1965).

[2] C. Caroli, P.-G. de Gennes, J. Matricon, Phys. Lett **9**, 307 (1964).

[3] J. Bardeen, R. Kümmel, A.E. Jacobs, L. Tewordt, Phys. Rev. **187**, 556 (1969).

[4] D. Rainer, J.A. Sauls, D. Waxman, Phys. Rev. B **54**, 10094 (1996).

[5] B. Jankó, J.D. Shore, Phys. Rev. B **46**, 9270-9273 (1992), T.C. Hsu, Physica C **213**, 305 (1993), Yu-Dong Zhu, Fu-Chun Zhang, H.D. Drew, Phys. Rev. B **47**, 586-588 (1993).

[6] N. B. Kopnin, JETP Lett. **27**, 391 (1978), N. B. Kopnin, G.E. Volovik, Phys. Rev. Lett. **79**, 1377 (1997), N. B. Kopnin, Phys. Rev. B **57**, 11775-11785 (1998)

[7] G. Eilenberger, Z. Phys. **214**, 195 (1968).

[8] A. I. Larkin, Y. N. Ovchinnikov, Sov. Phys. JETP **28**, 1200 (1969), Sov. Phys. JETP **41**, 960 (1976), Sov. Phys. JETP **46**, 155 (1977).

[9] G. M. Eliashberg, Sov. Phys. JETP **34**, 668 (1972).

[10] Y. Nagato, K. Nagai, J. Hara, J. Low Temp. Phys. **93**, 33 (1993).

[11] N. Schopohl, K. Maki, Phys. Rev. B **52**, 490 (1995).

[12] M. Eschrig, Ph.D. thesis (1997), Bayreuth University; cond-mat/9804330. (unpublished)

[13] L.P. Gorkov, N.B. Kopnin, Sov. Phys.-Usp. **18**, 496-513 (1975), S.N. Artemenko, A.F. Volkov, Sov. Phys.-Usp. **22**, 295 (1979).

[14] D. I. Khomskii, A. Freimuth, Phys. Rev. Lett. **75**, 1384 (1995), M. V. Feigel'man *et al*, JETP Lett. **62**, 834 (1995), G. Blatter, M. Feigel'man, V. Geshkenbein, A. I. Larkin, A. van Otterlo, Phys. Rev. Lett. **77**, 566 (1996).

[15] There is also a contribution to the current density from the "anomalous" Green's function which is not shown here. The spectral response shown in Fig. 3 dominates the dissipative current density in the core, while the anomalous response contributes primarily to the reactive response at low frequencies. For more detail see Ref. 12